

Numerical and Experimental Prediction of Lamb Wave Scattering from Horizontal Notch

ŠOFER Michal^{1,a}, FERFECKI Petr^{1,2,b}, FUSEK Martin^{1,c}, ŠOFER Pavel^{3,d}
and LIČKOVÁ Dagmar^{1,e}

¹ Department of Applied Mechanics, Faculty of Mechanical Engineering, VŠB-TU Ostrava, 17. listopadu 15/2172, 708 33 Ostrava-Poruba, Czech Republic

² IT4Innovations National Supercomputing Center, VŠB-Technical University of Ostrava, Studentská 6231/1B, 708 33 Ostrava-Poruba, Czech Republic

³ Department of Control Systems and Instrumentation, Faculty of Mechanical Engineering, VŠB-TU Ostrava, 17. listopadu 15/2172, 708 33 Ostrava-Poruba, Czech Republic

^amichal.sofer@vsb.cz, ^bpetr.ferfecki@vsb.cz, ^cmartin.fusek@vsb.cz, ^dpavel.sofer@vsb.cz, ^edagmar.lickova@vsb.cz

Keywords: Lamb wave, Wave scattering, Wavelet analysis, Orthogonality relation

Abstract: The presented paper deals with the topic of experimental and numerical prediction of energy transmission and reflection coefficients in the case of Lamb wave scattering on a two-millimetre deep and two-millimetre wide horizontal notch milled in a three-millimetre thick aluminium sheet. The paper contains the description of the experimental and numerical approaches, which were used for obtaining the above-mentioned coefficients. Great emphasis is also placed on the mutual comparison of results between these approaches as well as clarification of non-compliance of the results for particular Lamb wave modes.

Introduction

Lamb waves, as one of the types of guided waves, are extensively used for inspecting large structures as well as for structure health monitoring (SHM) [1]. These waves are one of the types of guided waves, which can exist only in geometries with a finite thickness such as plates, rods, or tubes [2]. Thanks to the ability to travel over long distances without much attenuation, an interaction of Lamb waves with particular types of geometric discontinuities has been an important topic of research [3-6]. In practice, the most challenging thing is in many cases the signal processing process related to the identification of the discontinuity type present in the inspected geometry [7]. Generally, the higher the number of Lamb wave modes present in the geometry, the more information related to a potentially present defect will be available. The level of post-processing complexity rapidly increases with the increasing number of present Lamb wave modes [8]. In many practical applications, we are often forced to utilize first two low-order Lamb wave modes at most. The main aim of the proposed paper is to present an experimental method, incorporation of the wavelet transform [9], for estimating energy reflection and transmission coefficients of low-order Lamb modes (A0/S0 mode), which are scattered by 2 mm wide and 2 mm deep vertical notch milled in 3 mm thick aluminum sheet. For subsequent verification of the obtained results, a hybrid method based on FEM approach and incorporation of orthogonality relation [8] is used.

Experimental Method for Scattering Coefficients Evaluation

The experiments were carried out on a three-millimetre thick aluminum sheet with the dimensions of 560 x 600 mm with a two-millimetre wide, two-millimetre deep and three hundred-millimetre long vertical notch milled on the top surface of the aluminum sheet (see Fig. 1). The coefficients were determined with respect to incident A0 Lamb mode, which has been excited by a focused air-coupled UT probe (Starmans PLF 19-012-T/F 120 kHz). The reflected and transmitted Lamb wave modes were detected by DWC B454 acoustic emission sensor, suitable for modal acoustic emission analysis. The Vallen AMSY-6 acoustic emission system served as a data acquisition unit as well as a signal generator. A five-cycle sinusoidal tone burst of 400 V_{peak-peak} and the central frequency of 150 kHz (Fig. 2) have been used as a driving signal for the above-mentioned air coupled transducer.

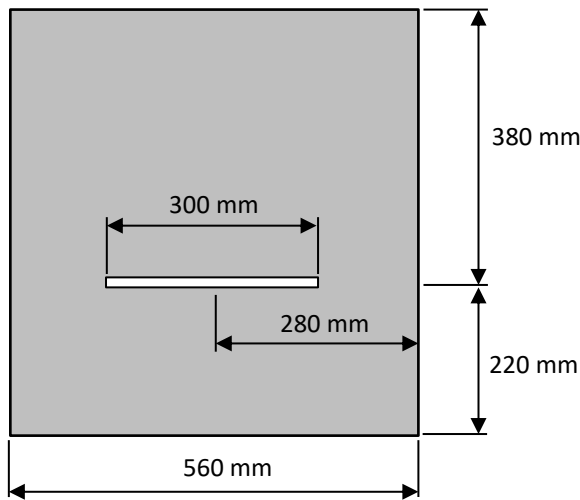


Fig.14 Schematic representation of the aluminum sheet including the position of the notch

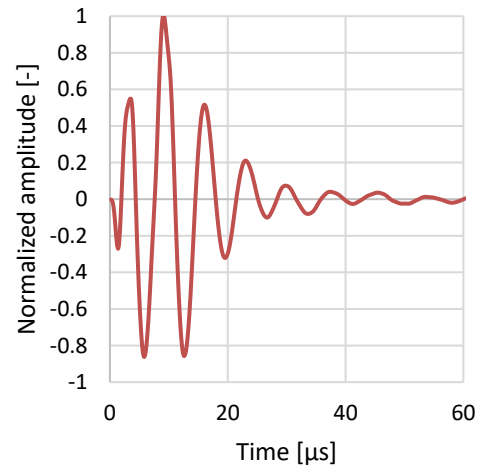


Fig.2 Driving signal for wave excitation

For proper generation of the incident A0 mode, the air coupled transducer has been placed into the positioning frame, which allows us to precisely adjust the exact position within four axes. The angle α (Fig. 3) can be derived using Snell's law:

$$\alpha = \arcsin \frac{c_{air}}{c_{phase}}, \quad (1)$$

where c_{air} is the speed of longitudinal wave in air (suppose 0.33 mm/μs) and c_{phase} is the phase velocity of the A0 mode in the aluminium plate of the given dimensions and material properties, which arise from the defined values of longitudinal and transversal speeds. Due to the discrepancy between the frequency of the driving signal and the resonant frequency of the transmitter, there is a need to determine the frequency of the generated A0 mode in order to retrospectively modify the angle α . In the first step, we suppose that the frequency of the generated A0 mode will be around 130 kHz. The A0 phase velocity is then equal to 1.69 mm/μs and finally, the value of angle α is equal to 11.1 deg. Subsequently, we will measure the frequency of the generated A0 mode in the aluminium plate, the value of which was 140 kHz. Then, we have to repeatedly determine the phase velocity for the 140 kHz A0 mode and finally calculate the resulting value for the excitation angle, which is equal to 10.6 deg. The sensor layout depended on whether we wanted to measure the transmission or the energy reflection coefficients. The following figure summarizes the two used different configurations. The diagram in Fig. 3 to the left displays the configuration used for estimation

of transmission coefficients. The transmitter is placed in front of the vertical notch, while the receiver is placed at a sufficient distance from the notch in order to ensure a proper separation of the transmitted A0 and S0 modes from each other. For estimation of energy reflection coefficients, a configuration in the figure to the right has been used. Again, the distance between the notch and the receiver had to be such that a proper separation of the reflected A0 and S0 modes is ensured.

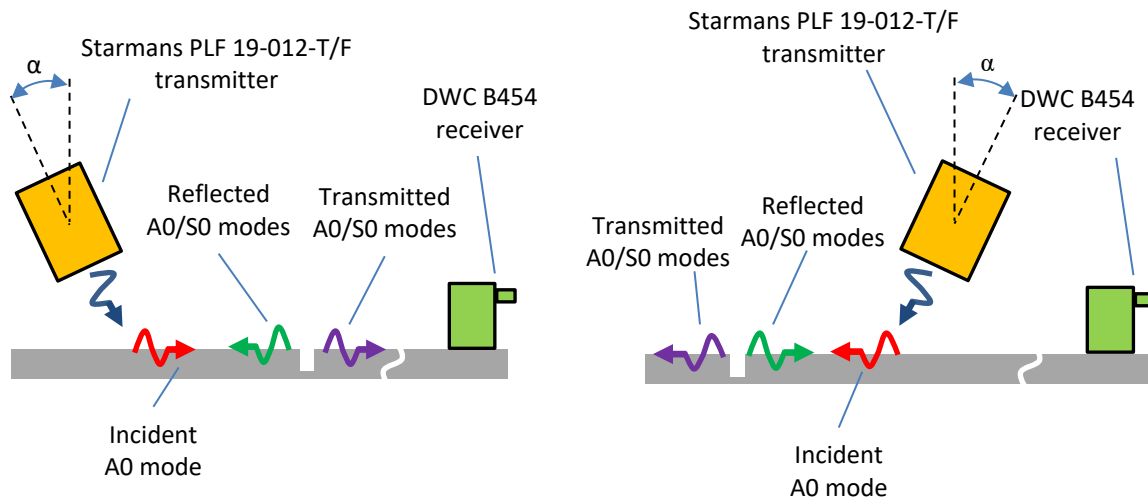


Fig.3 Left - configuration for estimation of the transmission coefficients; Right - configuration for estimation of the reflection coefficients

The calculation of the energy transmission and reflection coefficients was realized on the basis of time amplitude records of guided waves. Figures 4 and 5 display the time record in the case of the reflected and transmitted A0/S0 modes including the back-wall reflection from the plate's free end. The time amplitude records were, with regard to a better clarity, normalized.

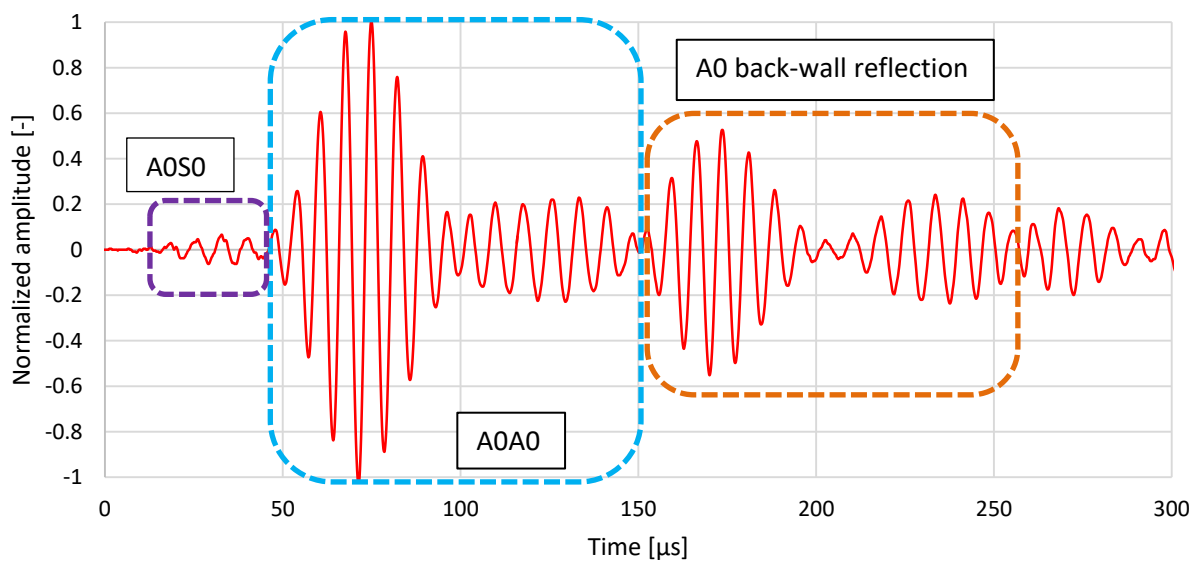


Fig.4 Time amplitude records of the reflected A0/S0 modes

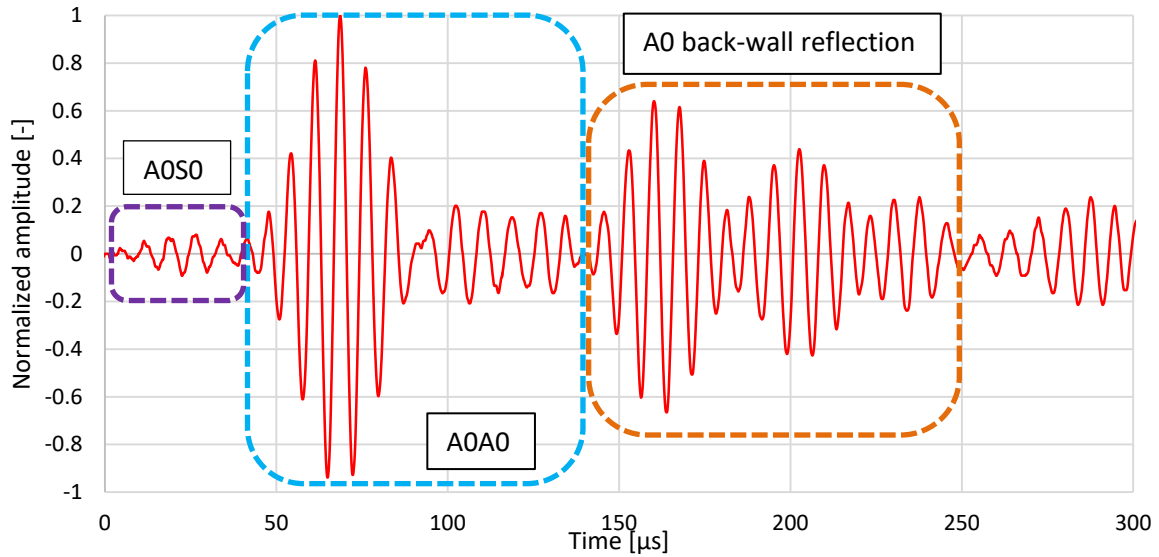


Fig.5 Time amplitude records of transmitted A0/S0 modes

The calculation process of the energy scattering coefficients includes the estimation of the energy related to the incident mode the value of the coefficient in itself is referred to. Therefore, a reference time amplitude record of the A0 mode (Fig. 6), which has propagated at the same path corresponding to the distance between the notch and the excitation point, has to be obtained.

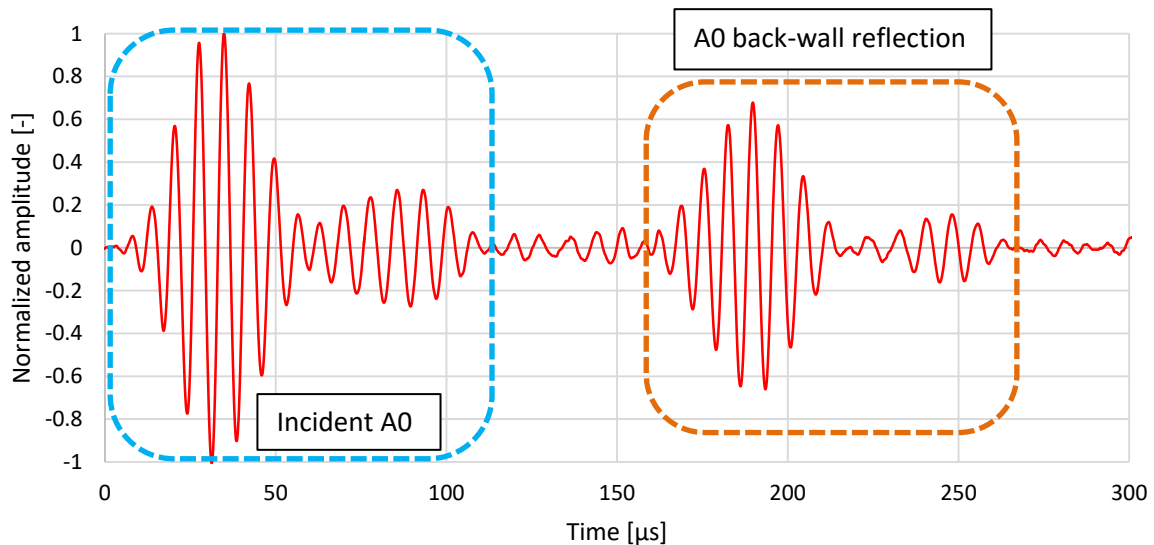


Fig.6 Time amplitude records of the reference A0 mode

After analysis and identification of the reflected and transmitted A0/S0 modes in the signal recordings (Figs. 4-6) were performed, a continuous wavelet transform using a Morlet mother wavelet function [9] was applied on the time amplitude records. In the following step, a projection of the desired part of the time-frequency spectrum belonging to the transmitted mode has to be performed into the frequency-max($c_{WT}(t, f)$) plane, where $c_{WT}(t, f)$ expresses the continuous wavelet transform coefficient, which depends on time t and frequency f . The frequency-max(c_{WT}) representation can be further used for final calculation of the power of a particular mode using the Parseval's theorem [10]:

$$P = \int_{t_1}^{t_2} |c_{WT_{MAX}}(t, f)|^2 dt, \quad (2)$$

where $c_{WT_MAX}(t, f)$ is the projected wavelet coefficient into the frequency-max(c_{WT}) plane and t_1 and t_2 express the time interval of occurrence of scattered Lamb wave mode, for which the time-averaged power has to be determined. It has to be noted that the wavelet coefficients displayed in Figs. 7 and 8 were normalized in order to achieve a better scale representation and has not been used for the previous computations.

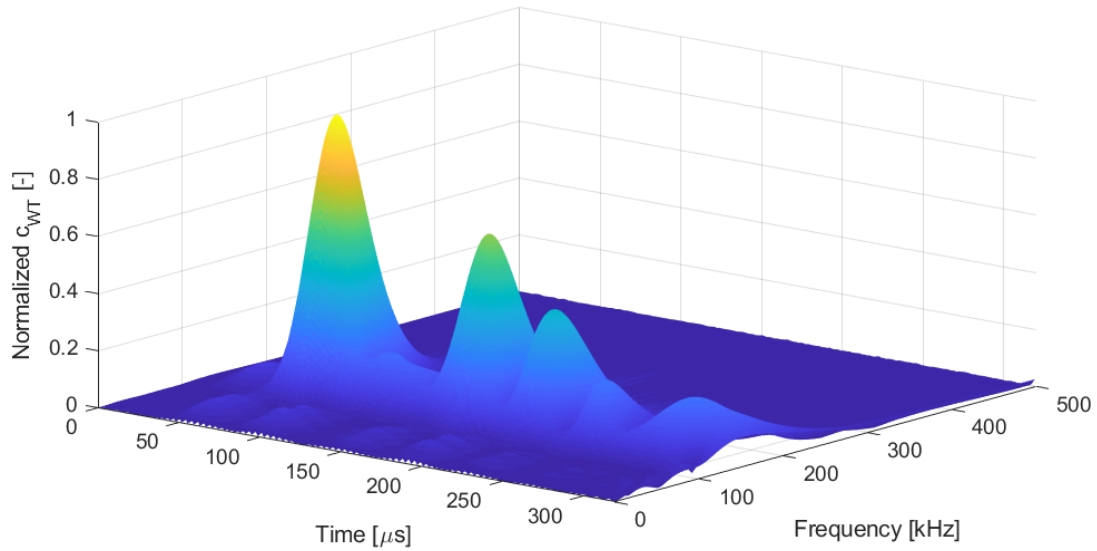


Fig.7 Calculated c_{WT} coefficients over the time-frequency domain in the case of the transmitted A0/S0 modes

The procedure of power calculation has to be carried out for each scattered mode ($S0_{ref}$, $S0_{trans}$, $A0_{ref}$, $A0_{trans}$) as well as for the incident A0 mode. Finally, the energy transmission/reflection coefficients can be computed as follows:

$$k_{S0ref} = \frac{P_{S0ref}}{P_{A0inc}}, k_{A0ref} = \frac{P_{A0ref}}{P_{A0inc}}, k_{S0trans} = \frac{P_{S0trans}}{P_{A0inc}}, k_{A0trans} = \frac{P_{A0trans}}{P_{A0inc}}, \quad (3)$$

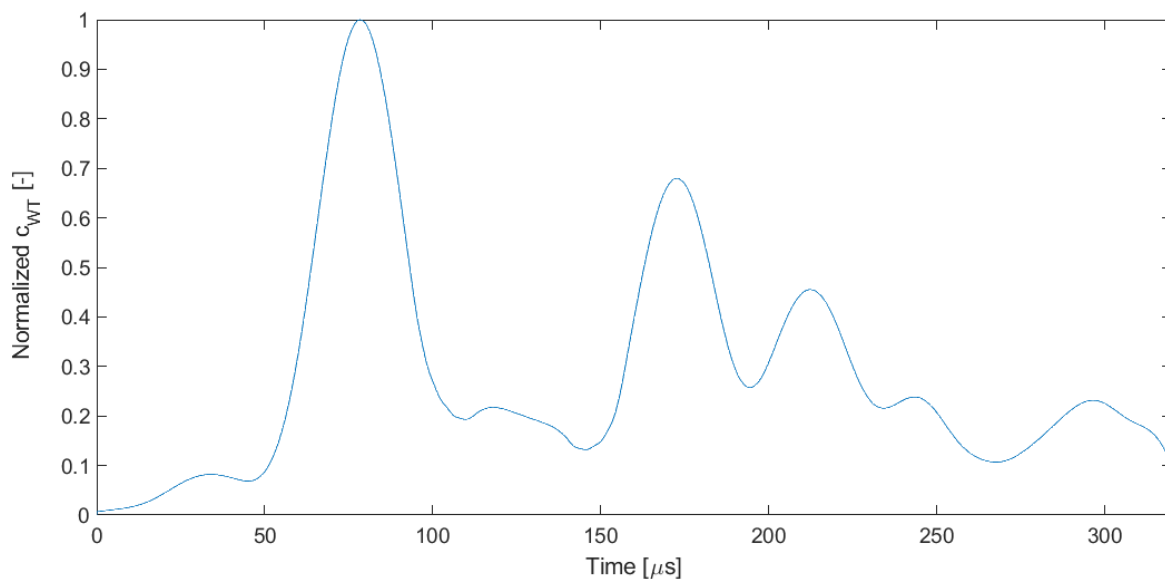


Fig.8 Normalized c_{WT_MAX} coefficients in the frequency-max(CWT coefficient) plane

where k_{S0ref} is the reflection coefficient of the reflected S0 mode, k_{A0ref} is the reflection coefficient of the reflected A0 mode, $k_{A0trans}$ is the transmission coefficient of the transmitted A0 mode, $k_{S0trans}$ is the transmission coefficient of the transmitted S0 mode, P_{S0ref} is the time-averaged power of the reflected S0 mode, P_{A0ref} is the time-averaged power of the reflected A0 mode, $P_{A0trans}$ is the time-averaged power of the transmitted A0 mode, $P_{S0trans}$ is the time-averaged power of the transmitted S0 mode and P_{A0inc} is the time-averaged power of the incident A0 mode.

Numerical Method for Scattering Coefficients Evaluation

Currently, there is a number of more or less complex methods for evaluation of scattering coefficients related to the interaction of Lamb waves with geometric discontinuities [1,6,8]. In this article, a modal extraction method based on an orthogonal property of Lamb modes has been used [8]. By means of combining the knowledge of the orthogonal property with information related to the through-thickness displacements and stress distribution, it is possible to derive the energy transmission and reflection coefficients for any present Lamb mode. A certain disadvantage lies in the need to determine the stress and displacement fields in the close vicinity of the discontinuity, for which the FEM method must be used in most cases [8]. For this case study, the stress and displacement fields were predicted using the COMSOL software. The FE simulation was realized in the frequency domain in order to obtain the above-mentioned through-thickness displacements and stress distribution in front of and above the discontinuity (vertical notch). The generation of the incident mode has been realized with the use of locally applied excitation of normal force with a Gaussian-windowed spatial distribution by the following function [8]:

$$F(x, f) = F_0 e^{-ikx} e^{\frac{A(x-x_0)^2}{B^2}}, \quad (4)$$

where F_0 (set at 100 N) represents the amplitude of the excitation force, k is the wavenumber, x refers to the spatial coordinate, A (set at 30 mm) defines the width of the excitation zone, and B (set at 60 mm) defines its length. The wavenumber of the incident A0 mode is a function of material properties, thickness of the plate as well as a function of the frequency of the wave. The wavelet analysis showed that the frequency of the excited A0 mode propagating in unloaded aluminium plate with the thickness of 3 mm is equal to 137 kHz with respect to the above-mentioned excitation method, i.e. combination of the used transmitter and the driving signal. In the next step, the wavenumber k for the A0 mode of frequency-thickness value equal to 0.411 MHz mm has to be determined for the material parameters explicitly expressed by means of transversal and longitudinal wave speeds. Figure 9 displays the scheme of the FE model the displacements and stress distribution were obtained from. The PML abbreviation expresses the Perfectly Matched Layer property, which is an artificial absorbing layer option available in the COMSOL software. The PML property enables us to minimize the dimensions of the model including the elimination of the back-wall reflection at the same time. After the data extraction, a method based on an orthogonal property of Lamb modes can be applied in order to evaluate the energy transmission and reflection coefficients.

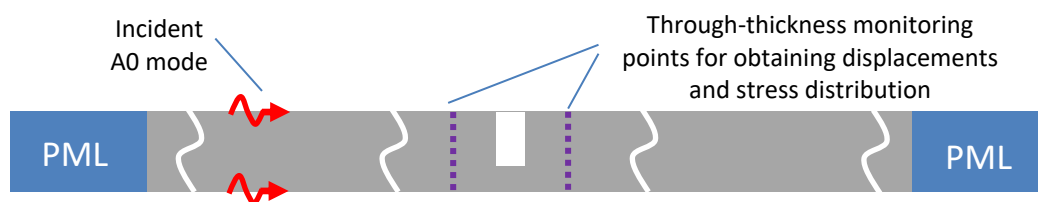


Fig.9 Scheme of the FE model for obtaining displacements and stress distribution

Results and Discussion

Two methods were used in order to evaluate the energy transmission and reflection coefficients in the case of Lamb wave scattering on a two-millimetre deep and two-millimetre wide horizontal notch milled in a three- millimetre thick aluminium sheet. As the incident wave, the A0 mode of Lamb wave was chosen especially for its sensitivity to such type of defects. The experimental method consisted of the measurement of the reflected and transmitted time amplitude records, which have been subjected to subsequent wavelet analysis in order to calculate the time-average power of the selected wave modes using Parseval's theorem [10]. In order to prove the experimental results, a hybrid method incorporating the FE method and the modal extraction method based on an orthogonal property of Lamb modes were used. The results of both approaches are summarized in Table 1.

Tab.1 Measured and computed results of the transmission/reflection coefficients

Transmission/reflection coefficients	Experimental method incorporating wavelet transform	Hybrid method incorporating the FE method and modal extraction method
k_{S0ref} [%]	0.30	13.9
k_{A0ref} [%]	44.1	39.7
$k_{S0trans}$ [%]	0.50	16.0
$k_{A0trans}$ [%]	25.5	30.6
Energy balance [%]	70.4	100.2

It is obvious that the hybrid method exhibits perfect results in terms of energy balance criterion. The experimental approach, on the other hand, reports a loss of one-third of the energy mainly caused by almost zero values of scattering coefficients related to the S0 Lamb wave mode. The reason for such disagreement lies in the wave structure of A0 and S0 modes having the frequency·thickness parameter of 0.411 MHz·mm.

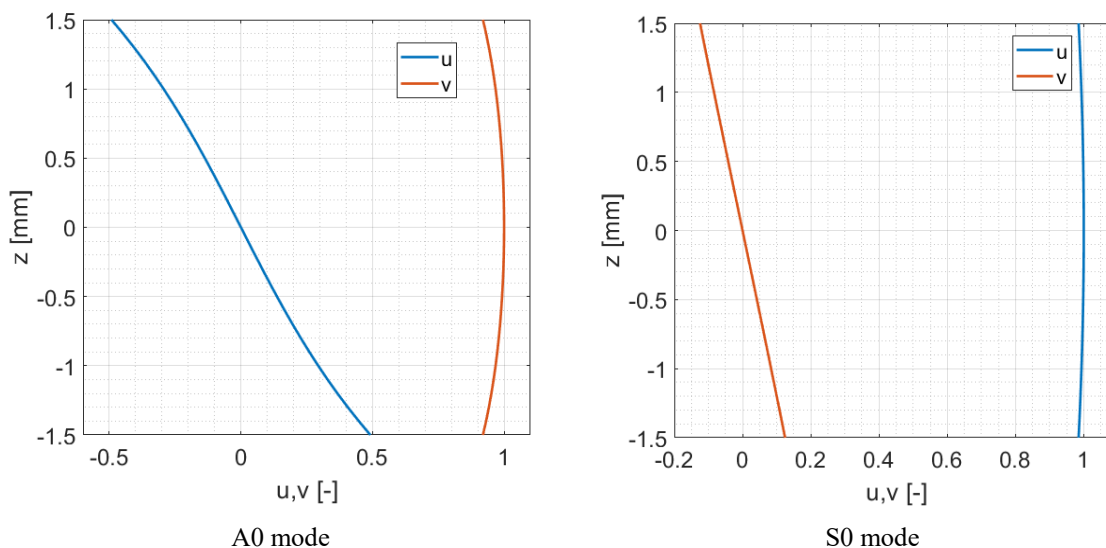


Fig.10 Normalized through-thickness displacements along x (u) and z axis (v)

Figure 10 displays the normalized through-thickness displacements u and v along x and z axis, respectively. The A0 mode of the frequencythickness parameter of 0.411 MHz·mm shows relatively large values of through-thickness displacement in z direction compared to through-thickness in x direction, which is a favourable situation for standard contact

piezoelectric transducers sensitive to longitudinal vibration. On the other hand, the S0 mode with the mentioned frequency-thickness parameter exhibits dominant displacements along x axis, while the displacement in z axis is more than five times smaller.

Therefore, the S0 mode will be obviously disadvantaged thanks to displacement ratio and its structure resulting in the predominant amplitudes of through-thickness displacement in x direction. This fact is, however, taken into account in the case of the modal extraction method, which incorporates both of the displacement components into its calculations. We can also notice that the values of transmission and reflection coefficients related to the A0 mode are very close to each other. The rate of the conformity between the experimental and numerical approaches therefore strongly depends on the types of Lamb modes they are working with.

Conclusion

The main aim of the proposed paper was to present the practical view on the usability of the experimental approach, which incorporates the wavelet transform as a tool for calculation of the scattering coefficients of low-order Lamb modes. The experimental approach has been tested on a simple vertical notch, and the results were then confronted with the hybrid method incorporating the FE method and the modal extraction method, which is based on an orthogonal property of Lamb modes. The mutual conformity between these two approaches depends mainly on the structure of considered wave modes the scattering coefficients are evaluated for. The experimental approach, however, proved to be a solid performer in terms of predicting the scattering coefficients for A0 mode. A deeper study of the mutual relationship between the particular low-order Lamb mode and the detectability for higher values of frequency-thickness product is also considered.

Acknowledgement

This work was supported by Specific Research (SP2018/63) and by The Ministry of Education, Youth and Sports from the National Programme of Sustainability II (LQ1602). The support is acknowledged. The authors would also like to thank the Starmans electronics Ltd. company for the provided ultrasonic probes and devices.

References

- [1] B. Poddar, V. Giurgiutiu, Complex modes expansion with vector projection using power flow to simulate Lamb waves scattering from horizontal cracks and disbonds, *J. Acoust. Soc. Am.* 140 (2016) 2123-2133.
- [2] T.N. Grigsby, E.J. Tajchman, Properties of Lamb Waves Relevant to the Ultrasonic Inspection of Thin Plates, *IRE Trans. Ultrason. Eng.* 8 (1961) 26-33.
- [3] F. Feng, J. Shen, J. Deng, Q. Wang, Analytical Solution of Lamb Wave Scattering at Plate End, *Advanced Materials Research* 199-200 (2011) 949-952.
- [4] J.L. Rose, *Ultrasonic Waves in Solid Media*, Cambridge University Press, Cambridge, 2002.
- [5] G. Shkerdin, C. Glorieux, Interaction of Lamb modes with an inclusion, *Ultrason.* 53 (2013) 130-140.
- [6] F. Feng, J. Shen, S. Lin, Scattering matrices of Lamb waves at irregular surface and void defects, *Ultrason.* (2012) 760-766.

- [7] D. N. Alleyne, P. Cawley, The Interaction of Lamb Waves with Defects, *IEEE Trans. Ultrason., Ferroelectrics and Frequency Control* 39 (1992) 381-397.
- [8] L. Moreau, M. Castaings, B. Hosten, An orthogonality relation-based technique for post-processing finite element predictions of waves scattering in solid waveguides, *J. Acoust. Soc. Am.* 120 (2006) 611-620.
- [9] H. Suzuki, T. Kinjo, Y. Hayashi, M. Takemoto, K. Ono, Wavelet Transform of Acoustic Emission Signals, *J. Acoust. Em.* 14 (1996) 69-84.
- [10] L. M. Surhone, M. T. Tennoe, S. F. Henssonow, *Parseval's Theorem*, Betascript Publishing, 2010.